Theoretical and experimental researches on continuous box girder bridges

Autor(en): **Konishi, Ichiro / Komatsu, Sadao / Fukumoto, Yuhshi**

Objekttyp: **Article**

Zeitschrift: **IABSE publications = Mémoires AIPC = IVBH Abhandlungen**

Band (Jahr): **19 (1959)**

PDF erstellt am: **30.04.2024**

Persistenter Link: https://doi.org/10.5169/seals-16953

Theoretical and Experimental Researches on Continuous Box Girder Bridges

Etude théorique et expérimentale des ponts à poutres continues en caisson

Theoretische und experimentelle Untersuchung von durchlaufenden Kastenträgerbrücken

ICHIRO KONISHI
Prof. Dr. Eng., Kyoto University, Kyoto

SADAO KOMATSU
Osaka City University, Osaka

YUHSHI FUKUMOTO
Kyoto University, Kyoto

Introduction

Continuous box girder bridges with steel deck have their statical and structural features to satisfy the following items required for the economical design of the bridges:

1. to distribute the stresses three-dimensionally under possible loading conditions;
2. to resist effectively against sectional forces such as bending moment, shearing force and twisting moment under the loading conditions, and
3. to display the statical features of thin-walled structures.

Therefore, a two-dimensional stress analysis by the ordinary method is not suitable for the stress analysis of continuous box girder bridges with stiffened thin-walled plates.

This paper deals theoretically with the stress analysis of the continuous box girder bridges from the view points mentioned above and clarified that the measured three-dimensional stress distributions can be explained theoretically by the torsion-bending theory in which warping of the cross-section of the bridge under the eccentric loadings is especially emphasized.

Theoretical Stress Analysis

The stress analysis and design calculation of simple box girder bridges by using the torsion-bending theory were presented by the authors previously [1]. The extended method with the torsion-bending theory on the continuous box girder bridges will be described in this section.

Thin-walled beams of closed cross-section such as box girder have large torsional rigidity and they give much influences upon the uniformity of stress in main girder and of load distribution on two main girders.

Diffused bicouples due to the restrained warping under the eccentric loadings occur at the intermediate supports of the continuous box girder bridges, and these diffused bicouples and bending moment of the elementary beam theory form sectional forces to keep the continuity at the intermediate supports of the beam. Twisting moment applied only to a certain span influences the other spans because of diffused bicouples occurred at the intermediate supports. On the stress analysis of the continuous box girder bridges not only torsional rigidity but also torsion-bending rigidity must be taken into account to explain the mutual relations between adjacent spans accurately. And these behaviors indicated above are far different from those of simple box girder bridges.

The torsion-bending theory may be written in the following form for the twisting moment $\mathfrak{M}(x)$ per unit length acting on the cross-section at distance x from the origin (fig. 1).

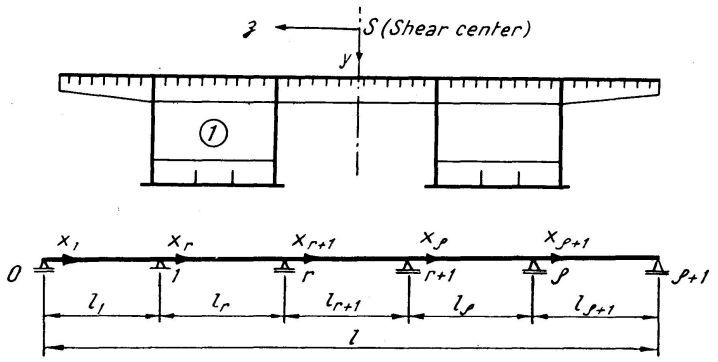

Fig. 1.

$$E\,C_w\frac{d^4\Phi}{dx^4}-K\frac{d^2\Phi}{dx^2}=\mathfrak{M}(x), \tag{1}$$

in which Φ is the angle of rotation of the cross-section at distance x, K the torsional rigidity, and EC_w the torsion-bending rigidity.

The formulæ K and EC_w are given as follows:

$$K=2\cdot 2\tilde{q}_1 F_1 G+\sum\tfrac{1}{3}G\,b\,t^3, \tag{2}$$

where G is shearing modulus, F_1 the mean of the areas enclosed by the outer

and the inner boundaries of the cross-section of the box girder, $\tilde{q}_1$ the torsion function and defined as $\tilde{q}_1 = \frac{q_1}{\frac{d\Phi}{dx} G}$ in which q_1 is St. Venant shear flow in simple torsion, b and t are width and thickness of the open cross-sections.

$$C_w = \int_F W_s^2 t \, ds, \tag{3}$$

in which W_s, the warping function, is given by

$$W_s = \frac{w_s}{\frac{d\Phi}{dx}} = -\int_0^s r_s \, ds + \int_0^s \frac{\tilde{q}_1}{t} \, ds, \tag{4}$$

where w_s is warping, r_s the distance between the shear center and the center line of the thin-walled sections.

Using the notation

$$\alpha_r = \sqrt{\frac{K_r}{E C_{w,r}}}, \tag{5}$$

the angle of rotation Φ_r of the r-th span can be solved from eq. (1) with the boundary condition (13).

$$\Phi_r = \frac{1}{\alpha_r^2}\left\{\frac{C_{w,r-1}}{C_{w,r}} \mathfrak{A}_{r-1} \frac{\sinh \alpha_r (l_r - x_r)}{\sinh \alpha_r l_r} + \mathfrak{A}_r \frac{\sinh \alpha_r x_r}{\sinh \alpha_r l_r}\right\} + A_r x_r + B_r + \theta_r, \tag{6}$$

in which $\mathfrak{A}_{r-1}$, $\mathfrak{A}_r$, A_r and B_r are constants of integration, which can be determined from the boundary conditions. θ_r is the angle of rotation of simple box girder bridge of the r-th span under the same loading on the r-th span of continuous box girder bridges.

Derivatives of eq. (6) are given as follows:

$$\frac{d\Phi_r}{dx_r} = \frac{1}{\alpha_r}\left\{-\frac{C_{w,r-1}}{C_{w,r}} \mathfrak{A}_{r-1} \frac{\cosh \alpha_r (l_r - x_r)}{\sinh \alpha_r l_r} + \mathfrak{A}_r \frac{\cosh \alpha_r x_r}{\sinh \alpha_r l_r}\right\} + \frac{d\theta_r}{dx_r} + A_r, \tag{7}$$

$$\frac{d^2\Phi_r}{dx_r^2} = \frac{C_{w,r-1}}{C_{w,r}} \mathfrak{A}_{r-1} \frac{\sinh \alpha_r (l_r - x_r)}{\sinh \alpha_r l_r} + \mathfrak{A}_r \frac{\sinh \alpha_r x_r}{\sinh \alpha_r l_r} + \frac{d^2\theta_r}{dx_r^2}, \tag{8}$$

$$\frac{d^3\Phi_r}{dx_r^3} = \alpha_r\left\{-\frac{C_{w,r-1}}{C_{w,r}} \mathfrak{A}_{r-1} \frac{\cosh \alpha_r (l_r - x_r)}{\sinh \alpha_r l_r} + \mathfrak{A}_r \frac{\cosh \alpha_r x_r}{\sinh \alpha_r l_r}\right\} + \frac{d^3\theta_r}{dx_r^3}. \tag{9}$$

θ_r in eq. (6) is given as follows for the four types of eccentric loading (fig. 2):

(1) $$\theta_r = \frac{\zeta_r \sinh \alpha_r x_r}{\alpha_r^4 \sinh \alpha_r l_r}(1 - \cosh \alpha_r l_r) + \frac{\zeta_r}{\alpha_r^4}\left(\cosh \alpha_r x_r - 1 - \frac{\alpha_r^2}{2} x_r^2\right) + \frac{\zeta_r l_r}{2\alpha_r^2} x_r, \tag{10}$$

$$(2)\quad \theta_r = \frac{\zeta_r \sinh \alpha_r x_r}{\alpha_r^4 \sinh \alpha_r l_r}[1-\cosh \alpha_r (l_r-c_r)] + \frac{\zeta_r (l_r-c_r)^2}{2\alpha_r^2 l_r} x_r + \frac{\zeta_r}{\alpha_r^4}\left[\cosh \alpha_r (x_r-c_r) - 1 - \frac{\alpha_r^2 (x_r-c_r)^2}{2}\right] \cdot U(x_r-c_r),$$

$$(3)\quad \theta_r = \frac{-\xi_r \sinh \alpha_r (l_r-c_r)}{\alpha_r^3 \sinh \alpha_r l_r} \sinh \alpha_r x_r + \frac{\xi_r (l_r-c_r)}{\alpha_r^2 l_r} x_r + \frac{\xi_r}{\alpha_r^3}[\sinh \alpha_r (x_r-c_r) - \alpha_r (x_r-c_r)] \cdot U(x_r-c_r), \tag{10}$$

$$(4)\quad \theta_r = \frac{-\eta_r \sinh \alpha_r (l_r-c_r)}{\alpha_r^3 \sinh \alpha_r l_r} \sinh \alpha_r x_r + \frac{\eta_r (l_r-c_r)}{\alpha_r^2 l_r} x_r + \frac{\eta_r}{\alpha_r^3}[\sinh \alpha_r (x_r-c_r) - \alpha_r (x_r-c_r)] \cdot U(x_r-c_r),$$

where

$$\xi_r = W\left(B-\frac{a}{2}\right)\frac{a}{EC_w}, \qquad \eta_r = P\frac{(B-a)}{EC_w}, \qquad \zeta_r = w_0\left(B-\frac{a}{2}\right)\frac{a}{EC_w},$$

$U(x_r-c_r)$: Unit step function.

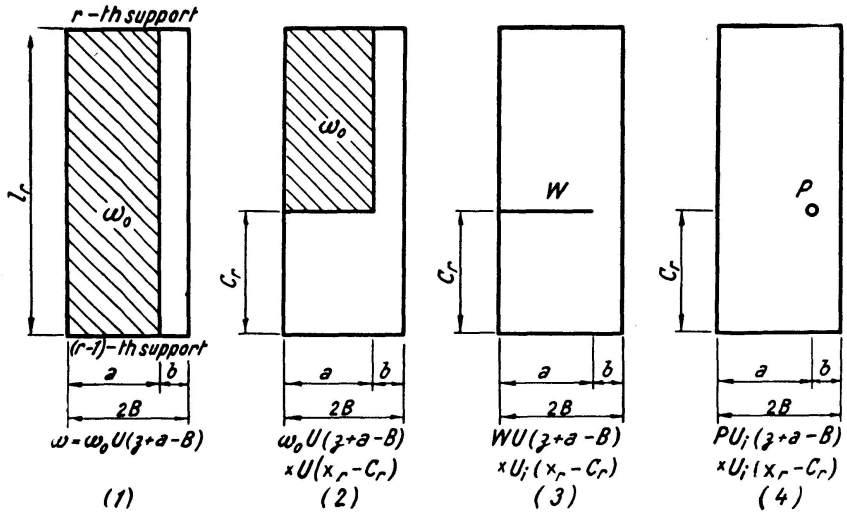

Fig. 2.

$\frac{d\theta_r}{dx_r}$, $\frac{d^2\theta_r}{dx_r^2}$ and $\frac{d^3\theta_r}{dx_r^3}$ in eqs. (7) through (9) are given by derivatives of eqs. (10) for the four types of eccentric loading respectively.

Conditions of continuity at the intermediate supports are:

$$[\Phi_r]_{x_r=l_r} = [\Phi_{r+1}]_{x_{r+1}=0} = 0, \tag{11}$$

$$\left[\frac{d\Phi_r}{dx_r}\right]_{x_r=l_r} = \left[\frac{d\Phi_{r+1}}{dx_{r+1}}\right]_{x_{r+1}=0}, \tag{12}$$

$$\left[C_{w,r}\frac{d^2\Phi_r}{dx_r^2}\right]_{x_r=l_r} = \left[C_{w,r+1}\frac{d^2\Phi_{r+1}}{dx_{r+1}^2}\right]_{x_{r+1}=0} \tag{13}$$

and at point 0 and $(\rho+1)$ of both ends of beams are:

$$[\Phi_1]_{x_1=0} = 0, \qquad [\Phi_{\rho+1}]_{x_{\rho+1}=l_{\rho+1}} = 0, \tag{14}$$

$$\left[\frac{d^2\Phi_1}{dx_1^2}\right]_{x_1=0} = 0, \quad \left[\frac{d^2\Phi_{\rho+1}}{dx_{\rho+1}^2}\right]_{x_{\rho+1}=l_{\rho+1}} = 0. \tag{15}$$

There are $4(\rho+1)$'s unknown constants in eq. (6), $4(\rho+1)$'s boundary and continuity conditions in eqs. (11) through (15). Hence all of the constants of integration can be determined as follows.

A_r and B_r are determined from the eqs. (11) and (14)

$$A_r = \frac{1}{\alpha_r^2 l_r}\left(\frac{C_{w,r-1}}{C_{w,r}}\mathfrak{A}_{r-1} - \mathfrak{A}_r\right), \tag{16}$$

$$B_r = \frac{1}{\alpha_r^2}\left(-\frac{C_{w,r-1}}{C_{w,r}}\mathfrak{A}_{r-1}\right). \tag{17}$$

From eqs. (15)

$$\mathfrak{A}_0 = \mathfrak{A}_{\rho+1} = 0. \tag{18}$$

Substituting eqs. (7) and (16) into the boundary condition (12), the following expression is obtained

$$\begin{aligned}
&\frac{C_{w,r-1}}{C_{w,r}}\frac{1}{\alpha_r^2 l_r}\left(1-\frac{\alpha_r l_r}{\sinh \alpha_r l_r}\right)\mathfrak{A}_{r-1} \\
&+\left\{\frac{1}{\alpha_r^2 l_r}(\alpha_r l_r \coth \alpha_r l_r - 1) + \frac{C_{w,r}}{C_{w,r+1}}\frac{1}{\alpha_{r+1}^2 l_{r+1}}(\alpha_{r+1} l_{r+1}\coth \alpha_{r+1} l_{r+1} - 1)\right\}\mathfrak{A}_r \\
&+\frac{1}{\alpha_{r+1}^2 l_{r+1}}\left(1-\frac{\alpha_{r+1} l_{r+1}}{\sinh \alpha_{r+1} l_{r+1}}\right)\mathfrak{A}_{r+1} = \left[\frac{d\theta_{r+1}}{dx_{r+1}}\right]_{x_{r+1}=0} - \left[\frac{d\theta_r}{dx_r}\right]_{x_r=l_r}, \\
&\qquad (r = 1, 2, \ldots, \rho).
\end{aligned} \tag{19}$$

Eq. (19) shows ρ's simultaneous linear equation in $\mathfrak{A}_r$, ρ's unknown constants of integration, and its form is analogous to that of Clapeyron's three moment equation. The right-hand side of eq. (19) corresponds to the terms of loading. The first term of that side indicates the angle of rotation per unit length at the r-th support due to the loading condition of the $(r+1)$-th span assumed as the simple box girder bridge, and the second term of that side shows the angle of rotation per unit length at the r-th support of the r-th span. And these values can be determined by derivatives of eqs. (10) substituting $x_r = l_r$ and $x_{r+1} = 0$.

Substituting the values A_r, B_r, $\mathfrak{A}_{r-1}$ and $\mathfrak{A}_r$ from eqs. (16), (17) and (19) in eq. (6), the angle of rotation Φ_r in the r-th span of the continuous box girder bridges can be obtained.

Normal stress σ and shearing stress τ over any cross-section can be analized as follows by using eqs. (7), (8) and (9):

$$\sigma = \sigma_b + \sigma_w, \qquad \tau = \tau_b + \tau_s + \tau_w. \tag{20}$$

Stresses σ_b and τ_b in bending are:

$$\sigma_b = \frac{M}{I} y, \tag{21}$$

$$\tau_b = \frac{q_b}{t} = \frac{1}{t}(\bar{q}_b + S), \tag{22}$$

in which

$$\bar{q}_b = \frac{Q}{I} \int_0^s y t \, ds, \qquad S = -\frac{\oint \frac{\bar{q}_b}{t} ds}{\oint \frac{ds}{t}}. \tag{23}$$

Q is the shearing force, I is the sectional moment of inertia of the box girder bridge, and $\int_0^s y t \, ds$ the moment with respect to the neutral axis of the portion of the cross-sectional area, and stresses τ_s, σ_w, and τ_w in torsion-bending are:

$$\tau_s = \frac{q_1}{t} = \frac{\tilde{q}_1 G \frac{d\Phi_r}{dx_r}}{t}, \tag{24}$$

$$\sigma_w = E \frac{\partial w_s}{\partial x} = E W_s \frac{d^2 \Phi_r}{dx_r^2}, \tag{25}$$

$$\tau_w = \frac{q_w}{t} = -\frac{E \frac{d^3 \Phi_r}{dx_r^3}}{t} \left[\int_0^s W_s t \, ds + S_w \right], \tag{26}$$

where

$$S_w = -\frac{\oint_1 \frac{\int_0^s W_s t \, ds}{t} ds}{\oint_1 \frac{ds}{t}}.$$

Numerical Example

Numerical example will be given for the stress distributions on the model of three-span continuous box girder bridge ($L = 75 + 100 + 75$ cm) manufactured by plastic material of polymethachrilmethyl, Acrylite, as shown in fig. 3.

Properties of material (at 8° C):

$$E = 3.65 \times 10^4 \text{ kg/cm}^2$$
$$G = 1.34 \times 10^4 \text{ kg/cm}^2$$
$$\nu = 0.36 \qquad (\epsilon < 0.13\%)$$

1. Shear center and q_h- and q_b-diagrams

The cross-section taking symmetry axis for y-axis, the shear center will be on that axis. We calculate the position of the shear center from eq. (27).

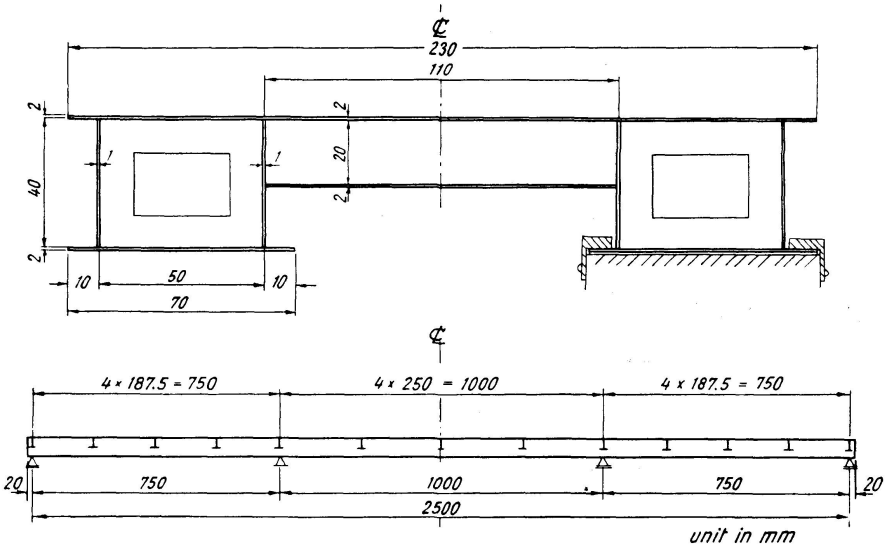

Fig. 3.

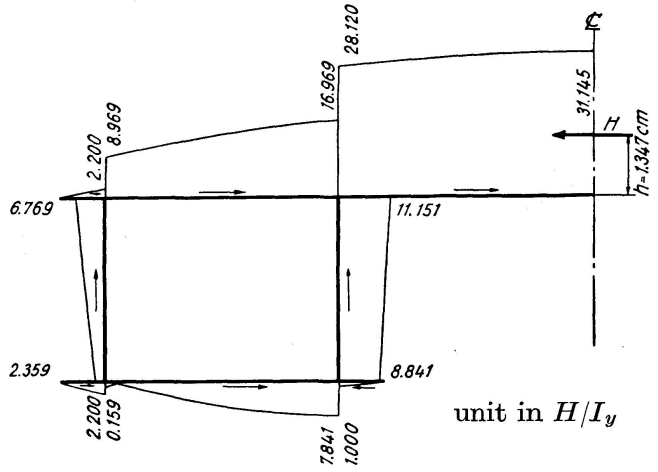

Fig. 4.

$$h = \frac{M_t}{H} = \frac{\int_F q_h r_c \, ds}{H}, \tag{27}$$

in which the horizontal force H is parallel to the z-axis and at such a distance h from the center line of the deck (point C) that twisting of the bridge does not occur, q_h the shear flow in bending due to the force H, and r_c the distance between the point C and the center line of the thin-walled sections.

Fig. 4 shows the shear flow q_h, and $\int_F q_h r_c \, ds = 688.863 \frac{H}{I_y}$ (kg·cm)

$$h = \frac{688.863 \dfrac{H}{I_y}}{H} = \frac{688.863}{511.44} = 1.347 \text{ cm}.$$

q_b-diagram: $q_b = \bar{q}_b + S$ in eqs. (23) are calculated as shown in fig. 5.

2. Torsion function $\tilde{q}_1$ and torsional rigidity K_r

Torsion function $\tilde{q}_1$ in eqs. (2) and (4):

$$\tilde{q}_1 = \frac{q_1}{G\dfrac{d\Phi_r}{dx_r}} = \frac{2F_1}{\oint_1 \dfrac{ds}{t}} = \frac{2\times 5.0\times 4.2}{2\left(\dfrac{5.0}{0.2}+\dfrac{4.2}{0.1}\right)} = 0.3134 \text{ cm}^2.$$

Torsional rigidity K_r in eq. (2):

$$\begin{aligned} K_r &= (2\cdot 2\tilde{q}_1 F_1 + \textstyle\sum \frac{1}{3} b t^3)\, G \\ &= \{2\times 2\times 0.3134\times 21 + \tfrac{1}{3}[0.2^3(5.5+1.0+1.0+1.0)]\}\, G \\ &= (26.328+0.227)\, G = 26.555\, G \text{ kg}\cdot\text{cm}^2. \end{aligned}$$

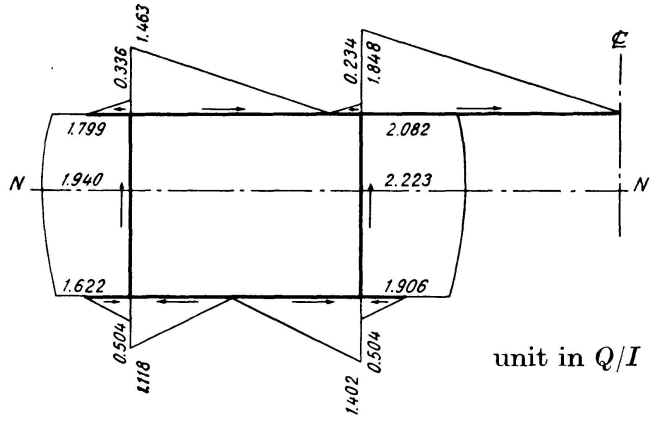

Fig. 5.

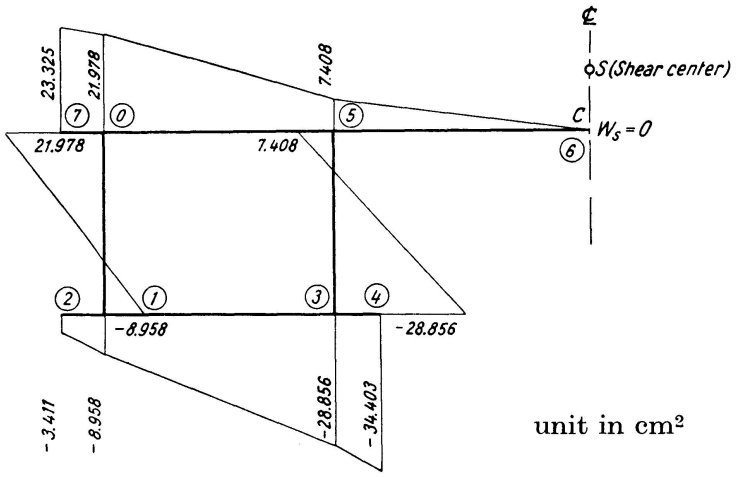

Fig. 6.

3. Warping function W_s.

Warping function W_s in eq. (4) is calculated as shown in table 1 and in fig. 6.

Table 1. Calculation of Warping Function W_s

Sections	$-\int_{i-1}^{i} r_s\,ds$	$-\int_{0}^{s} r_s\,ds$	$\int_{i-1}^{i} \frac{ds}{t}$	$\int_{i-1}^{i} \tilde{q}_1 \frac{ds}{t}$	$\int_{0}^{s} \tilde{q}_1 \frac{ds}{t}$	W_s (cm²)	Points
	0	0	—	—	—	0	6
6—5	$1.347 \times 5.5 = 7.408$	7.408	—	—	—	7.408	5
5—0	$1.347 \times 5.0 = 6.735$	14.143	$\frac{5.0}{0.2} = 25$	7.836	7.836	21.978	0
0—7	$1.347 \times 1.0 = 1.347$	15.490	—	—	7.836	23.325	7
0—1	$-10.500 \times 4.2 = -44.100$	-29.957	$\frac{4.2}{0.1} = 42$	13.164	20.999	- 8.958	1
1—3	$5.547 \times (-5.0) = -27.735$	-57.692	$\frac{5.0}{0.2} = 25$	7.836	28.836	-28.856	3
1—2	$5.547 \times 1.0 = 5.547$	-24.410	—	—	20.999	- 3.411	2
3—4	$5.547 \times (-1.0) = -5.547$	-63.239	—	—	28.836	-34.403	4

4. Torsion-bending rigidity $E C_{w,r}$ and α_r.

Warping function W_s varies linearly along the thin-walled sections and we calculate the torsion-bending rigidity $E C_{w,r}$ as shown in table 2.

$$E C_{w,r} = E \int_{i-1}^{i} W_s^2 t\,ds = E t_i \int_{0}^{\Delta s_i} \left(W_{i-1} + \frac{W_i - W_{i-1}}{\Delta s_i} s \right)^2 ds$$

$$= E \frac{t_i}{3} \Delta s_i (W_{i-1} W_i + W_i^2 + W_{i-1}^2)$$

$$= 2201.098\,E \text{ cm}^6.$$

And

$$\alpha_r = \sqrt{\frac{K_r}{E C_{w,r}}} = \sqrt{\frac{26.555\,G}{2201.098\,E}} = 0.0667 \text{ cm}^{-1}.$$

Substituting these values in eqs. (6) through (9), we obtain the values of Φ_r, $\frac{d\Phi_r}{dx_r}$, $\frac{d^2\Phi_r}{dx_r^2}$ and $\frac{d^3\Phi_r}{dx_r^3}$ in each case of four types of eccentric loading. Thus the stress distributions over any cross-section of the continuous box girder bridges can be determined from eqs. (20).

Fig. 7 shows the influence lines of normal stress σ at point S of the mid-span cross-section of center-span due to the eccentric loadings and also shows the same lines of the center-span assumed as the simple girder bridge.

Table 2. Calculation of C_w

Sections	W_{i-1}	W_i	$W_{i-1} \cdot W_i$	W_{i-1}^2	W_i^2	$\sum$	$\frac{t_i}{3} \Delta s_i$	$\int_{i-1}^{i} W_s^2 t\, ds$
0—1	21.978	- 8.957	-196.872	483.051	80.237	366.416	$\frac{0.1 \times 4.2}{3} = 0.140$	51.298
1—3	- 8.958	-28.856	258.482	80.237	832.691	1171.410	$\frac{0.2 \times 5.0}{3} = 0.333$	390.466
3—5	-28.856	7.408	-213.770	832.691	54.879	673.800	$\frac{0.1 \times 4.2}{3} = 0.140$	94.332
2—1	- 3.411	- 8.958	30.550	11.632	80.237	112.420	$\frac{0.2 \times 1.0}{3} = 0.067$	7.495
4—3	-34.403	-28.856	992.755	1183.587	832.691	3009.032	$\frac{0.2 \times 1.0}{3} = 0.067$	200.603
7—0	23.325	21.978	512.654	544.071	483.051	1539.775	$\frac{0.2 \times 1.0}{3} = 0.067$	102.652
0—5	21.978	7.408	162.817	483.051	54.879	700.747	$\frac{0.2 \times 5.0}{3} = 0.333$	233.580
5—6	7.408	0	0	54.879	0	54.879	$\frac{0.2 \times 5.5}{3} = 0.367$	20.122

$C_w = 2 \times 1100.549 = 2201.098$ (cm^6)

$\sum = 1100.549$

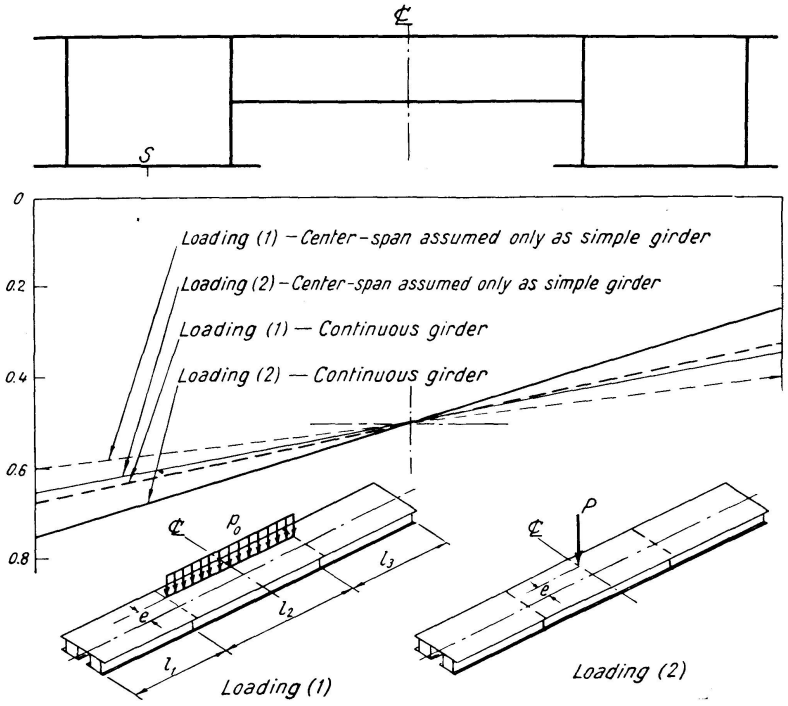

Fig. 7.

Experimental Stress Analysis

The test model is such as shown in fig. 3. Strains are measured by electric-resistance strain gages S_{21} (8 mm × 2 mm) and $R_{21}L$ (rosette), and deflections are by dial gages. The model is loaded directly with dead weight in the order 0 – 11.34 – 0 – 11.34 – 22.68 – 11.34 kg – 0.

Fig. 8 shows the experimental distributions of normal stress at Section

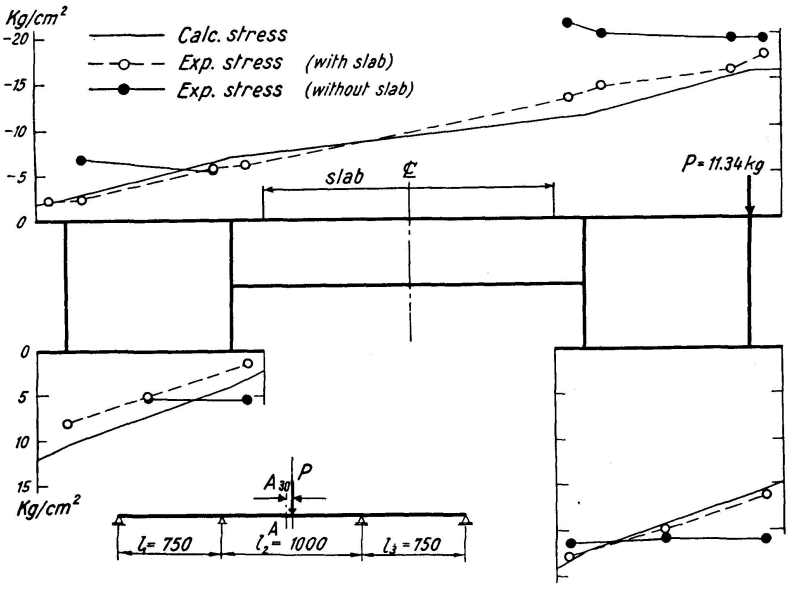

Fig. 8.

A–A of the center span. A load acts on the outside web plate of the mid-span cross-section. The stress distribution calculated by using the torsion-bending theory is also shown.

Fig. 9 shows an experimental distribution of normal stress at Section B–B of the intermediate support. The loading condition is the same one as shown in fig. 8.

Fig. 10 shows the influence lines of shearing stress at point R which is on the outer web plate of cross-sections C–C and D–D due to an eccentric loading at one-fourth cross-section of center-span.

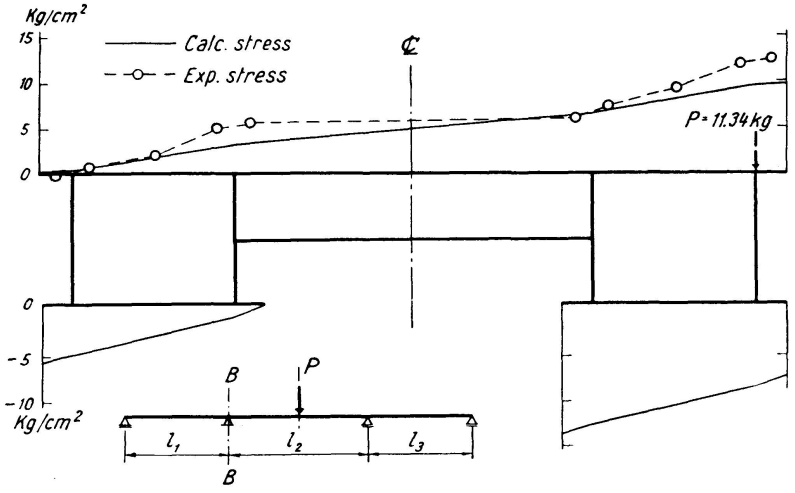

Fig. 9.

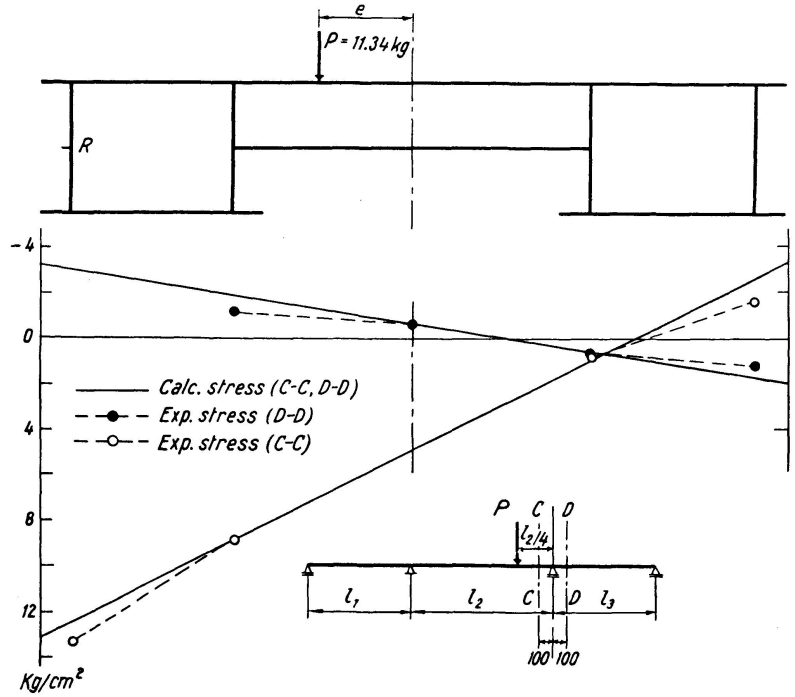

Fig. 10.

Conclusions

The following conclusions have been drawn:

1. the three-dimensional stress distributions of the continuous box girder bridges under the eccentric loadings can be obtained theoretically by using torsion-bending theory;
2. the external load on the bridge may be distributed on the two box girders of the continuous box girder bridges less sufficiently than on the simple box girder bridges;
3. the spanwise normal stress distribution on the steel deck varies continuously along the whole cross-section of the bridge, and these tendencies essentially differ from those of stress analyses as the grillage of beams, and
4. these results are also proved by the plastic model tests.

Reference

1. I. Konishi, S. Komatsu, and M. Ohashi, Stress analysis and calculation for design of composite box girder, Trans. of JSCE, No. 25, 1955.

Summary

This present paper deals theoretically with an analysis of the three-dimensional stress distribution of a continuous box girder bridge, and warping of the cross-section of the bridge under the eccentric loadings is especially emphasized. Experimental studies have been done by using a plastic model of Acrylite with a span length $L = 75 + 100 + 75$ cm.

The following conclusions have been drawn; (1) the three-dimensional stress distribution of the continuous box girder bridge under the eccentric loading is obtained theoretically, (2) the spanwise normal stress distribution on the steel deck varies continuously along the whole cross-section of the bridge, and (3) these results are also proved by the plastic model tests.

Résumé

L'auteur étudie la répartition théorique tridimensionnelle des contraintes dans un pont à poutres continues en caisson, en tenant particulièrement compte de la torsion de la section sous l'influence d'une charge excentrique. Il a d'autre part effectué des essais sur un modèle plastique en acrylite avec les portées de $75 + 100 + 75$ cm.

Il est arrivé aux conclusions suivantes:

— La répartition tridimensionnelle des contraintes dans un pont à poutres

continues en caisson sous l'effet d'une charge excentrique peut être déterminée théoriquement.
— La contrainte normale dans la direction longitudinale, pour la dalle métallique, varie d'une manière continue sur toute la section du pont.
— Ces résultats ont été confirmés par les essais.

Zusammenfassung

In dieser Abhandlung wird die theoretische, dreidimensionale Spannungsverteilung einer durchlaufenden Kastenträgerbrücke untersucht mit spezieller Berücksichtigung der Verdrehung des Querschnittes unter einem exzentrischen Lastangriff. Versuche wurden zusätzlich an einem Plastikmodell aus Acrylite mit den Spannweiten 75 + 100 + 75 cm durchgeführt.

Folgende Schlußfolgerungen werden gezogen:

— Die dreidimensionale Spannungsverteilung der durchlaufenden Kastenträgerbrücke unter exzentrischer Last kann theoretisch bestimmt werden.
— Die Normalspannung in Feldrichtung der stählernen Deckplatte variiert kontinuierlich über dem ganzen Brückenquerschnitt.
— Diese Resultate werden durch den Versuch bestätigt.